

STRUCTURAL
CHEMISTRY

ISSN 2053-2296

research papers

A bipyridine-ligated zinc(II) complex with bridging flavonolate ligation: synthesis, characterization, and visible-light-induced CO release reactivity

Shayne Sorenson,^a Marina Popova,^a Atta M. Arif^b and Lisa M. Berreau^{a*}

Received 14 February 2017

Accepted 2 August 2017

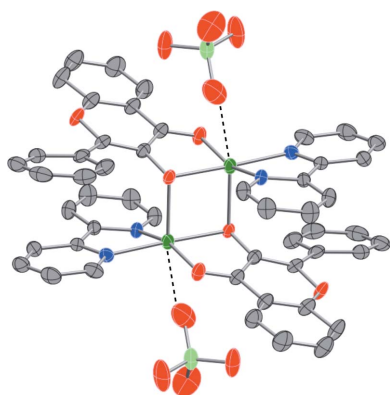
Edited by V. Langer, Chalmers University of Technology, Sweden

Keywords: zinc; flavonol; conductivity; carbon monoxide; nuclearity; crystal structure; CO release; synthetic models.**CCDC reference:** 1566131**Supporting information:** this article has supporting information at journals.iucr.org/c^aDepartment of Chemistry & Biochemistry, Utah State University, 0300 Old Main Hill, Logan, UT 84322-0300, USA, and^bDepartment of Chemistry, University of Utah, 315 S. 1400 E., Rm 1170, Salt Lake City, UT 84112-0850, USA.*Correspondence e-mail: lisa.berreau@usu.edu

Metal–flavonolate compounds are of significant current interest as synthetic models for quercetinase enzymes and as bioactive compounds of importance to human health. Zinc–3-hydroxyflavonolate compounds, including those of quercetin, kampferol, and morin, generally exhibit bidentate coordination to a single Zn^{II} center. The bipyridine-ligated zinc–flavonolate compound reported herein, namely bis(μ -4-oxo-2-phenyl-4*H*-chromen-3-olato)- $\kappa^3 O^3, O^3, O^4; \kappa^3 O^3, O^4: O^3$ -bis[(2,2'-bipyridine- $\kappa^2 N, N'$)zinc(II)] bis(perchlorate), $\{[Zn_2(C_{15}H_9O_3)_2(C_{10}H_8N_2)_2](ClO_4)_2\}_n$, (**1**), provides an unusual example of bridging 3-hydroxyflavonolate ligation in a dinuclear metal complex. The symmetry-related Zn^{II} centers of (**1**) exhibit a distorted octahedral geometry, with weak coordination of a perchlorate anion *trans* to the bridging deprotonated O atom of the flavonolate ligand. Variable-concentration conductivity measurements provide evidence that, when (**1**) is dissolved in CH₃CN, the complex dissociates into monomers. ¹H NMR resonances for (**1**) dissolved in *d*₆-DMSO were assigned *via* HMQC to the H atoms of the flavonolate and bipyridine ligands. In CH₃CN, (**1**) undergoes quantitative visible-light-induced CO release with a quantum yield [0.004 (**1**)] similar to that exhibited by other mononuclear zinc–3-hydroxyflavonolate complexes. Mass spectroscopic identification of the [(bpy)₂Zn(*O*-benzoylsalicylate)]⁺ ion provides evidence of CO release from the flavonol and of ligand exchange at the Zn^{II} center.

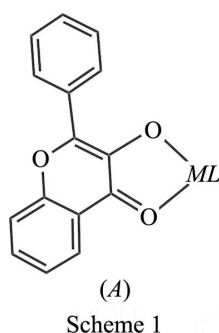
1. Introduction

Metal complexes of flavonols are of considerable current interest (Kasprzak *et al.*, 2015; Wei & Guo, 2014). Compounds of this class containing a 3-hydroxyflavonolate ligand have been investigated as models for quercetin dioxygenase enzymes [$M = Cu^I, Cu^{II}, Ni^{II}, Co^{II},$ and Fe^{II} : Speier *et al.*, 1990; Balogh-Hergovich *et al.*, 1991; Balogh-Hergovich, Kaizer, Speier, Argay & Parkanyi, 1999; Balogh-Hergovich, Kaizer, Speier, Fülöp & Parkanyi, 1999; Huang *et al.*, 2017; Kaizer *et al.*, 2004; Pap *et al.*, 2010; Grubel *et al.* 2010; Sun *et al.*, 2013, 2014*a,b*, 2017). Metal–flavonolate complexes can also exhibit biologically relevant properties that are important for human health. Examples include compounds that exhibit anticancer ($M = Ru^{II}$; Kurzwernhart, Kandioller, Bächler *et al.*, 2012; Kurzwernhart, Kandioller, Bartel *et al.*, 2012; Kurzwernhart *et al.*, 2013; Saraf *et al.*, 2014), antidiabetic ($M = Zn^{II}$; Vijayaraghavan *et al.*, 2012), and antioxidant (Pieniazek *et al.*, 2014; de Souza & de Giovanni, 2004) properties. Radiopharmaceuticals ($M = Re^I$; Schutte *et al.*, 2011) and light-induced CO releasing molecules ($M = Zn^{II}$; Grubel *et al.*, 2011, 2013) have also been developed based on metal–flavonolate structures. The 3-hydroxyflavonolate ligand typically coordinates in a bidentate



© 2017 International Union of Crystallography

manner to a single metal center [see (A) in Scheme 1]. Recently, we reported the first example of bridging flavonolate ligation in a dinuclear zinc complex using an extended flavonol ligand (Popova *et al.*, 2017). In this contribution, we report the synthesis and characterization of a zinc–3-hydroxyflavonolate (3-Hfl) complex having the empirical formula $[(\text{bpy})\text{Zn}(3\text{-Hfl})]\text{ClO}_4$ (bpy is 2,2'-bipyridine), (1) (Scheme 2). In the solid state, this complex contains symmetry-related $\mu\text{-}\eta^2\text{:}\eta^1\text{-}3\text{-hydroxyflavonolate}$ ligands bridging between Zn^{II} centers. When dissolved in acetonitrile, the cationic portion of this complex dissociates into mononuclear units, which undergo visible-light-induced CO release reactivity. The observed quantum yield for this reaction is similar to that found for $[(\text{TPA})\text{Zn}(3\text{-Hfl})]\text{ClO}_4$ [TPA is tris(pyridin-2-yl)methylamine] (Anderson *et al.*, 2014).



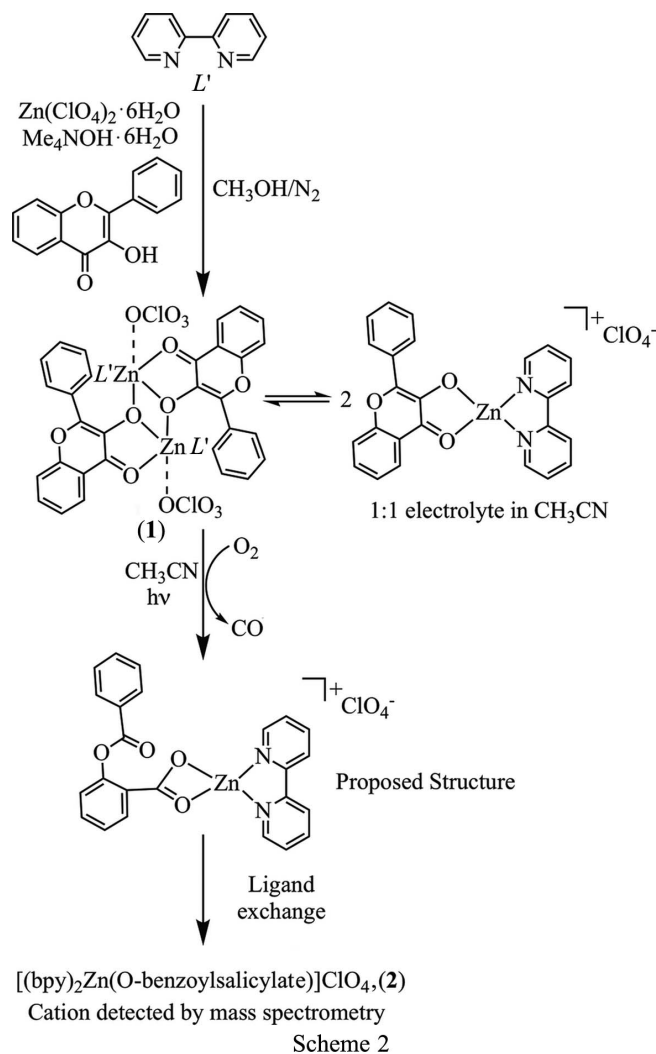
2. Experimental

2.1. General procedure

All experiments were performed in air. All reagents were obtained and used from commercial sources unless otherwise noted. ^1H NMR spectra were recorded on a JEOL ECX-300 MHz NMR spectrometer. ^1H NMR chemical shifts are reported in ppm (δ) relative to the chemical shift of the residual solvent ($d_6\text{-DMSO}$: δ 2.50 ppm; CD_3CN : δ 1.94 ppm). FT-IR spectra were collected using a Shimadzu FTIR-8400 spectrometer as KBr pellets. UV-Vis absorption spectra were collected using a HP8453 diode array spectrophotometer. Fluorescence emission spectra were collected using a Shimadzu RF-530XPC spectrometer, with the excitation wavelength corresponding to the absorption maximum of the complex. The excitation and emission slit widths were set at 3 nm. Conductance measurements were performed as described previously (Allred *et al.*, 2002). The 1:2 electrolyte standard $[(6\text{-Ph}_2\text{TPA})\text{Ni}(\text{CH}_3\text{CN})_2](\text{ClO}_4)_2$ (Szajna *et al.*, 2004) was prepared according to literature procedures. CO quantification measurements were performed under air as described previously (Grubel *et al.*, 2013). The reaction quantum yield for CO release from (1) was determined using ferrioxalate as a standard to measure photon flux (Hatchard & Parker, 1956; Kuhn *et al.*, 2004). Mass spectrometry data were collected at the University of California Riverside. Elemental analysis data were obtained by Atlantic Microlabs of Norcross, GA, using a PE2400 automatic analyzer.

Caution! Perchlorate salts of metal complexes containing organic ligands are potentially explosive. Only small amounts

of material should be prepared (~ 50 mg) and these should be handled with great caution (Wolsey, 1973).



2.2. Synthesis and crystallization of $[(\text{bpy})\text{Zn}(3\text{-Hfl})]\text{ClO}_4$, (1)

To a solution of 3-hydroxyflavone (50 mg, 0.21 mmol) in CH_3OH (3 ml) in a glass vial was added solid $\text{Me}_4\text{NOH}\cdot 5\text{H}_2\text{O}$ (38 mg, 0.21 mmol). The resulting mixture was stirred for 10 min at room temperature. In a separate reaction vessel, 2,2'-bipyridine (33 mg, 0.21 mmol) was combined with $\text{Zn}(\text{ClO}_4)_2\cdot 6\text{H}_2\text{O}$ (78 mg, 0.21 mmol) in CH_3OH (3 ml) and was stirred for 10 min. The two solutions were combined and the resulting solution stirred for an additional 1 h. The solvent was removed under reduced pressure and the remaining solid dissolved in CH_2Cl_2 . The solution was filtered through a celite/glass wool plug to remove Me_4NClO_4 and $\text{Zn}(3\text{-Hfl})_2$ (yellow precipitate). The filtrate was collected and left open to air at room temperature for 24 h, which produced crystals suitable for single-crystal X-ray diffraction (yield 21%). ^1H NMR ($d_6\text{-DMSO}$, 300 MHz): δ 8.75 (*br m*, 4H), 8.61 (*d*, $J = 6.9$ Hz, 2H), 8.21 (*br m*, 2H), 8.03 (*d*, $J = 6.2$ Hz, 1H), 7.81 (*t*, $J = 8.3$ Hz, 1H), 7.75 (*br m*, 3H), 7.57 (*t*, $J = 7.6$ Hz, 2H), 7.44 (*t*, $J = 7.2$ Hz, 1H), 7.39 (*t*, $J = 6.9$ Hz, 1H). FT-IR (KBr, cm^{-1}): 1580 ($\nu_{\text{C=O}}$); UV-Vis [CH_3CN , ϵ ($M^{-1}\text{cm}^{-1}$): 414 (19,000). Analysis calculated

Table 1
 Experimental details.

Crystal data	
Chemical formula	$[\text{Zn}_2(\text{C}_{15}\text{H}_9\text{O}_3)_2(\text{C}_{10}\text{H}_8\text{N}_2)_2] \cdot (\text{ClO}_4)_2$
M_r	1116.45
Crystal system, space group	Monoclinic, $P2_1/n$
Temperature (K)	150
a, b, c (Å)	10.6003 (2), 14.0573 (3), 15.8141 (2)
β (°)	104.0158 (10)
V (Å ³)	2286.33 (7)
Z	2
Radiation type	Mo $K\alpha$
μ (mm ⁻¹)	1.24
Crystal size (mm)	0.28 × 0.25 × 0.20
Data collection	
Diffractometer	Nonius KappaCCD
Absorption correction	Multi-scan (DENZO-SMN; Otwinowski & Minor, 1997)
$T_{\text{min}}, T_{\text{max}}$	0.722, 0.789
No. of measured, independent and observed [$I > 2\sigma(I)$] reflections	8971, 5225, 4417
R_{int}	0.016
$(\sin \theta/\lambda)_{\text{max}}$ (Å ⁻¹)	0.649
Refinement	
$R[F^2 > 2\sigma(F^2)], wR(F^2), S$	0.037, 0.093, 1.03
No. of reflections	5225
No. of parameters	341
No. of restraints	28
H-atom treatment	H-atom parameters constrained
$\Delta\rho_{\text{max}}, \Delta\rho_{\text{min}}$ (e Å ⁻³)	1.06, -0.51

Computer programs: COLLECT (Hoof, 1998), DENZO-SMN (Otwinowski & Minor, 1997), SIR97 (Altomare *et al.*, 1999), SIR2004 (Burla *et al.*, 2005), SHELXL2014 (Sheldrick, 2015), OLEX2 (Dolomanov *et al.*, 2009) and ORTEP-3 for Windows (Farrugia, 2012).

for $\text{C}_{25}\text{H}_{17}\text{ClN}_2\text{O}_7\text{Zn}$: C 53.79, H 3.07, N 5.02%; found: C 53.39, H 2.65, N 5.05%.

2.3. Refinement

Crystal data, data collection and structure refinement details are summarized in Table 1. The H atoms were assigned isotropic displacement coefficients [$U_{\text{iso}}(\text{H}) = 1.2U_{\text{eq}}(\text{C})$] and their positions were allowed to ride on their respective C atoms. The perchlorate anion is highly disordered and attempts at modeling the disorder over more than two sites were unsuccessful. Two positions (occupation ratio ~0.82:0.18) were defined for all atoms of this anion. The modeling of the perchlorate anion required the use of bond-similarity restraints (SADI) and displacement-ellipsoid constraints (EADP), as implemented in SHELXL2014 (Sheldrick, 2015).

2.4. Illumination of (1) with visible light – product identification

An acetonitrile solution of (1) (1.2 mM) was illuminated with 419 nm light for 24 h under aerobic conditions using a Luzchem photoreactor. The solution was brought to dryness under reduced pressure. The remaining solid was analysed by ¹H NMR, FT-IR, and ESI-MS. The ¹H NMR features are consistent with the presence of multiple species; FT-IR (KBr,

Table 2
 Selected geometric parameters (Å, °).

Zn1–O1	2.0448 (14)	Zn1–N1	2.0595 (18)
Zn1–O2	2.0315 (16)	Zn1–N2	2.0765 (18)
Zn1–O1 ⁱ	2.1353 (15)	Zn1–Zn1 ⁱ	3.0891 (5)
O2–Zn1–O1	81.87 (6)	N1–Zn1–N2	79.76 (7)
O2–Zn1–N1	98.67 (7)	O2–Zn1–O1 ⁱ	102.45 (6)
O1–Zn1–N1	177.08 (7)	O1–Zn1–O1 ⁱ	84.73 (6)
O2–Zn1–N2	161.55 (7)	N1–Zn1–O1 ⁱ	97.93 (6)
O1–Zn1–N2	98.81 (6)	N2–Zn1–O1 ⁱ	95.96 (6)

Symmetry code: (i) $-x + 1, -y + 1, -z + 1$.

cm⁻¹): 1725 ($\nu_{\text{C=O}}$); ESI-MS (CH₃CN): m/z calculated for $\text{C}_{34}\text{H}_{16}\text{N}_4\text{O}_3\text{Zn}$: 617.1167 [$M - \text{ClO}_4$]⁺; found: 617.1179. The FT-IR and ESI-MS data are consistent with a species having a [(bpy)₂Zn(*O*-benzoysalicylate)]⁺ cationic portion.

3. Results and discussion

3.1. Synthesis and structure of (1)

The synthesis of (1) was achieved *via* the admixture of equimolar amounts of 2,2'-bipyridine (bpy), Zn(ClO₄)₂·6H₂O, and Me₄N[3-Hfl] (3-Hfl is 3-hydroxyflavonolate) (Scheme 2). The synthesis is complicated by the formation of Zn(3-Hfl)₂, a highly insoluble yellow powder (Grubel *et al.*, 2010). Filtration to remove this by-product and crystallization from CH₂Cl₂ gave an average isolated yield for (1) of ~21% in the form of single crystals. Elemental analysis data are consistent with the proposed formulation of [(bpy)Zn(3-Hfl)]ClO₄, (1). Further

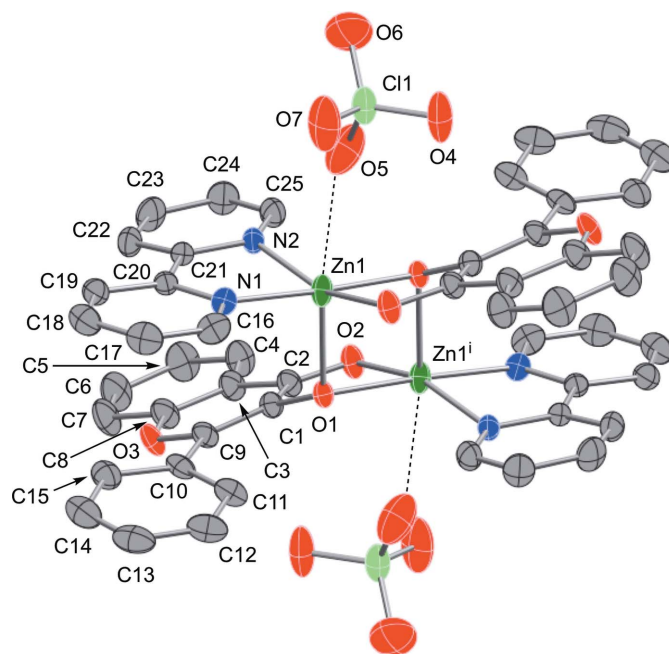


Figure 1
 The atom-numbering scheme of (1) (50% probability displacement ellipsoids). H atoms have been omitted for clarity. The O atoms of the perchlorate anions are disordered over two positions (occupation ratio ~0.82:0.18). Only one orientation is shown for clarity. [Symmetry code: (i) $-x + 1, -y + 1, -z + 1$.]

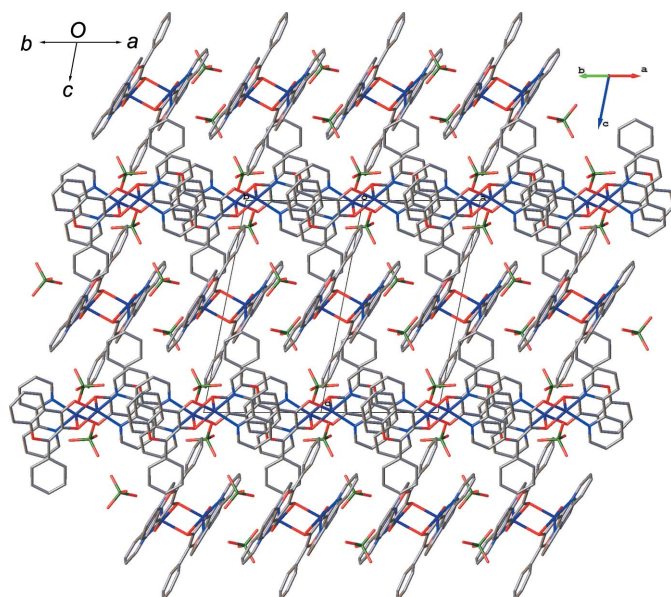


Figure 2
The molecular packing of **(1)**, viewed along [110]. H atoms have been omitted for clarity.

characterization of **(1)** was performed using single-crystal X-ray crystallography, ^1H NMR, FT-IR, UV-Vis, fluorescence, and conductivity measurements.

The asymmetric unit of **(1)** contains one Zn^{II} ion bonded to the N-atom donors of a 2,2'-bipyridine ligand and the ketone and deprotonated hydroxy O atoms of the flavonolate ligand in a distorted planar arrangement. An O atom of a perchlorate anion occupies one axial position. These combined structural features are similar to those found in $[(\text{bpy})\text{Cu}(3\text{-Hfl})]\text{ClO}_4$ (Lippai *et al.*, 1997). The differentiating feature of **(1)** is that the deprotonated hydroxy O1 atom bridges to an inversion-related Zn^{II} center at $(-x + 1, -y + 1, -z + 1)$ to create a dimer containing a planar Zn_2O_2 four-membered ring (see

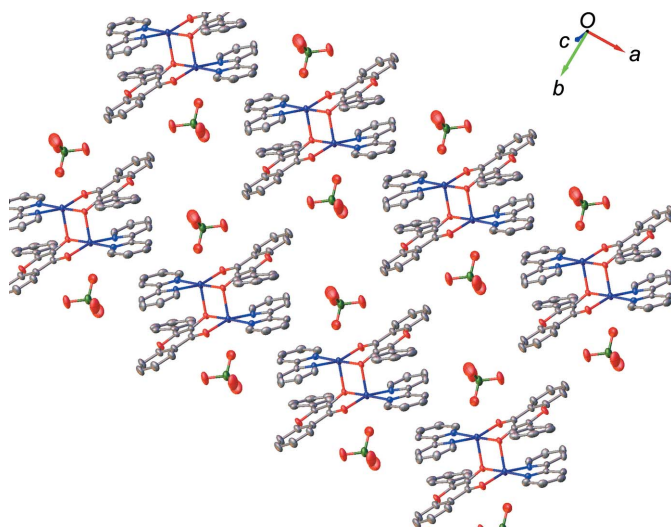


Figure 3
Offset stacking between molecular units within a column, viewed along $[\bar{1}27]$. Displacement ellipsoids drawn at the 50% probability level. H atoms have been omitted for clarity.

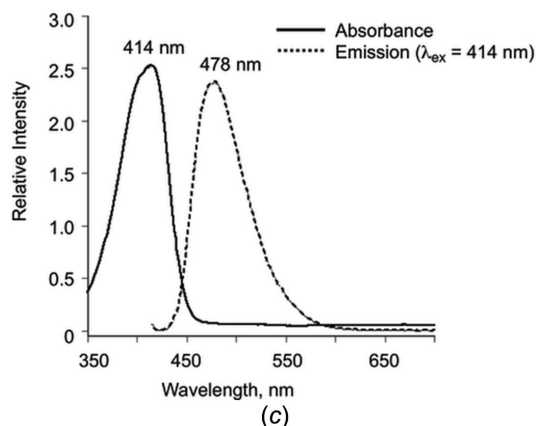
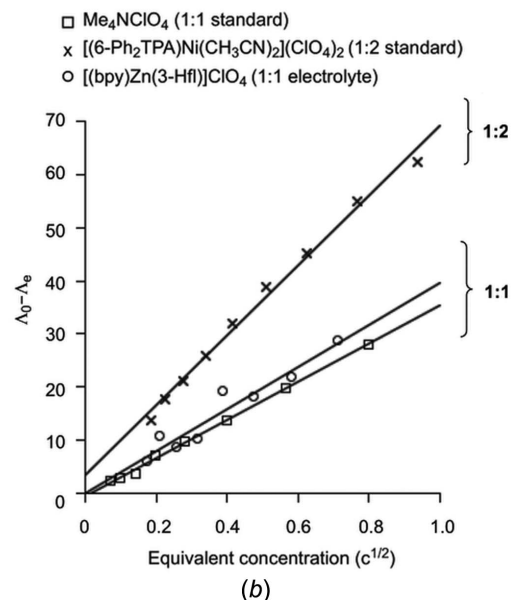
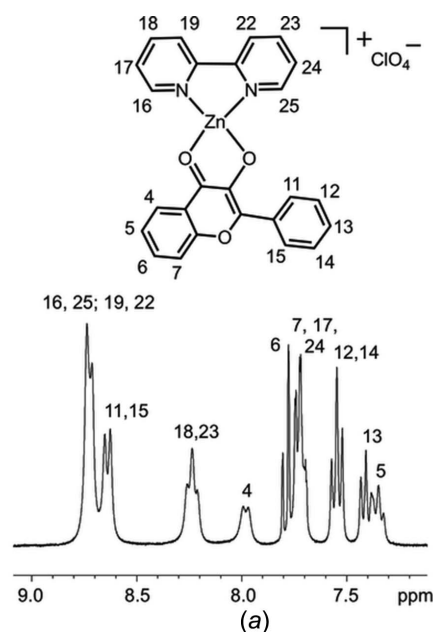


Figure 4
(a) (Top) The proton-containing ligands of one Zn^{II} center of **(1)**. (Bottom) ^1H NMR features in d_6 -DMSO, with assignments determined by HMQC. (b) Onsager plot of conductivity data for **(1)** in CH_3CN . (c) Absorption and emission spectra of **(1)** in CH_3CN .

Table 3

Parameters of selected offset-stacked interactions involving the aromatic rings of (**1**).

$Cg1$ is the centroid of the O3/C8/C3–C1/C9 ring, $Cg2$ that of the N1/C16–C20 ring, $Cg3$ that of the C3–C8 ring, and $Cg5$ that of the C10–C15 ring. CgI_{Perp} is the perpendicular distance of CgI on ring J , CgJ_{Perp} is the perpendicular distance of CgJ on ring I and Slippage is the distance between CgI and the perpendicular projection of CgJ on ring I .

CgI	CgJ	$Cg \cdots Cg$ distance (Å)	Dihedral angle (°)	CgI_{Perp} (Å)	CgJ_{Perp} (Å)	Slippage (Å)
$Cg1$	$Cg3^i$	3.4378 (12)	12.40 (1)	3.3692 (9)	–3.3317 (9)	0.848
$Cg2$	$Cg5^i$	3.5856 (14)	8.09 (12)	3.3794 (10)	3.5040 (11)	0.760
$Cg3$	$Cg4^i$	4.1065 (14)	10.49 (12)	3.3678 (9)	–3.6709 (11)	1.841
$Cg2$	$Cg3^{ii}$	3.8258 (13)	8.84 (11)	3.5192 (10)	–3.3228 (9)	1.896

Symmetry codes: (i) $-x + 1, -y + 1, -z + 1$; (ii) $-x + 2, -y + 1, -z + 1$.

Scheme 2). The dinuclear structure, including the weakly coordinated perchlorate anions and the atom numbering, is shown in Fig. 1. Selected bond lengths and angles are given in Table 2. Within each dinuclear unit, offset-stacked aromatic interactions, with centroid–centroid distances of 3.4378 (12) ($Cg1 \cdots Cg3^i$), 3.5856 (14) ($Cg2 \cdots Cg5^i$), and 4.1065 (14) ($Cg3 \cdots Cg4^i$) Å (Table 3) (Hunter & Sanders, 1990), are found

between arene rings of the flavonolate ligand and the pyridine rings of the 2,2'-bipyridine ligand on the other Zn^{II} center. The $Zn-O$ distances involving the flavonol keto and deprotonated O atoms are similar [$Zn1-O1 = 2.0448$ (14) Å and $Zn1-O2 = 2.0315$ (16) Å], as are the $Zn-N$ distances involving the bipyridine ligand [$Zn1-N1 = 2.0595$ (18) Å and $Zn1-N2 = 2.0765$ (18) Å]. The interaction involving the perchlorate anion is longer [$Zn1 \cdots O5 = 2.664$ (4) Å], but within the sum of the van der Waals radii of the atoms (2.79 Å; Bondi, 1964). The dinuclear cations form a one-dimensional chain in the solid state comprised of offset stacking-type interactions involving the bipyridyl ligands (Figs. 2 and 3) (Janiak, 2000). These interactions are characterized by a bipyridyl centroid–centroid distance of 3.8258 (13) Å ($Cg2 \cdots Cg3^{ii}$) (Table 3).

Complex (**1**) has some structural similarity in terms of the dinuclear metal core with complexes containing bridging maltolate-type ligands (Amatori *et al.*, 2014; Benelli *et al.*, 2013). A few examples of zinc complexes with bridging maltolate ligands have been reported (Petrus & Sobota, 2012*a,b*; Petrus *et al.*, 2013). Bridging 3-hydroxyflavonolate ligation akin to that identified in (**1**) has been proposed

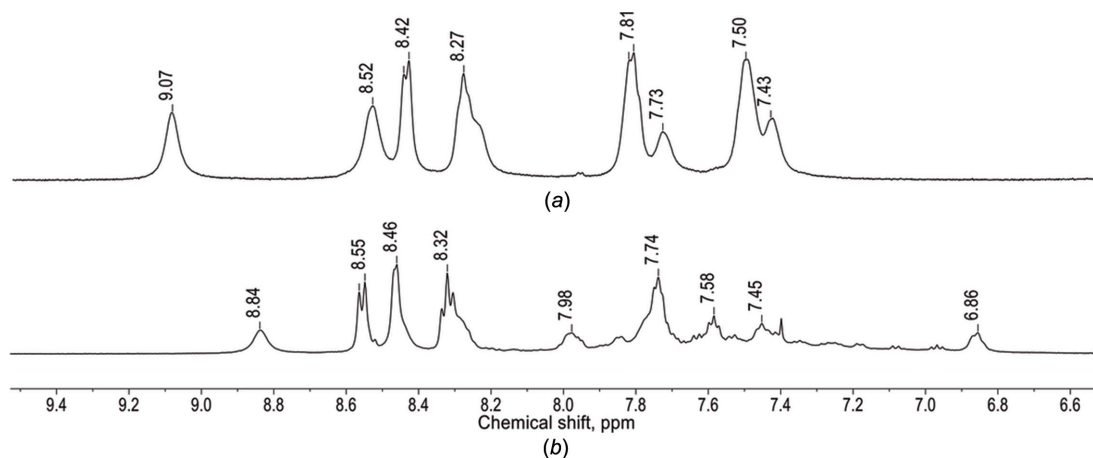


Figure 5
 ^1H NMR features of (**1**) (in CD_3CN) (a) before and (b) after exposure to visible light.

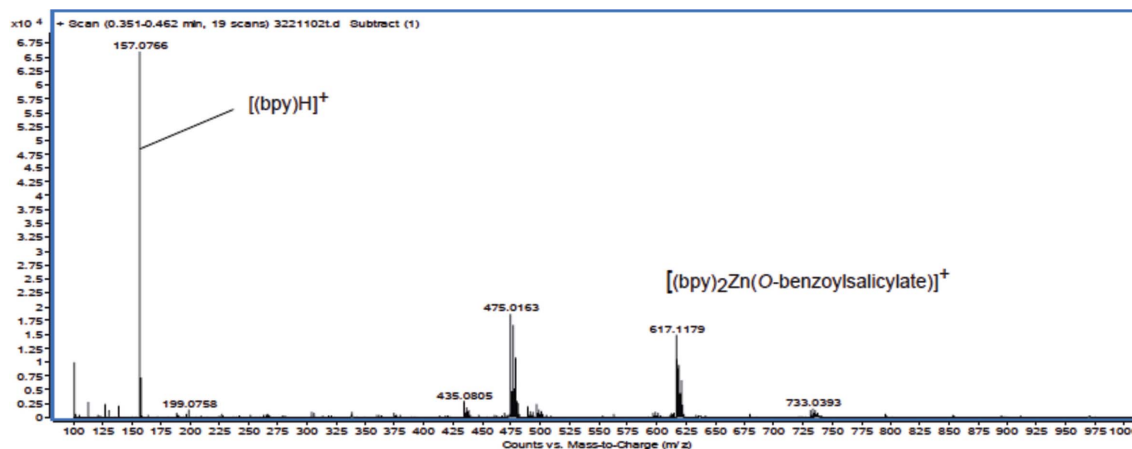


Figure 6
ESI-MS (CH_3CN) spectrum of the product mixture generated upon exposure of (**1**) to visible light in CD_3CN . Identification of the $[(\text{bpy})_2\text{Zn}(\text{O-benzoylsalicylate})]^+$ ion.

previously on the basis of flavonolate-ligand-exchange reactivity between metal centers (Grubel *et al.*, 2010).

3.2. Solution properties and visible-light-induced CO release reactivity

The ^1H NMR features of (**1**) in d_6 -DMSO are consistent with the presence of a 1:1 ratio of bpy and 3-hydroxy-flavonolate ligands (Fig. 4a). Assignment of the ^1H resonances was achieved *via* HMQC. When dissolved in acetonitrile, complex (**1**) exhibits conductivity properties consistent with dissociation of the dinuclear structure into a 1:1 electrolyte (Fig. 4b). Specifically, the slope of the Onsager plot for (**1**) matches that of the 1:1 standard Me_4NClO_4 and is clearly distinct from the 1:2 electrolyte $[(6\text{-Ph}_2\text{TPA})\text{Ni}(L)_2](\text{ClO}_4)_2$ ($L = \text{CH}_3\text{CN}$) (Szajna *et al.*, 2004). The observed absorption and emission properties of (**1**) (Fig. 4c) are similar to those found for other mononuclear zinc-3-hydroxyflavonolate complexes (Anderson *et al.*, 2014).

When illuminated with visible light ($\lambda = 419\text{ nm}$) under aerobic conditions, complex (**1**) undergoes quantitative visible-light-induced quantitative CO release [0.96 (4) equivalents]. This reaction occurs with a quantum yield of 0.004 (1), which is similar to that found for $[(\text{TPA})\text{Zn}(3\text{-Hfl})]\text{ClO}_4$ [0.006 (3); Anderson *et al.*, 2014]. The zinc-containing product generated was characterized by ^1H NMR (Fig. 5), ESI-MS (Fig. 6), and FT-IR. The ESI-MS shows a molecular ion at m/z 617.1179, which is consistent with a formulation of $[(\text{bpy})_2\text{Zn}(O\text{-benzoylsalicylate})]^+$, (**2**) (Scheme 2), and dioxxygenase-type CO release reactivity. The observation of this ion demonstrates the propensity for ligand exchange in this labile complex. The solid-state IR spectrum of (**2**) contains a $\nu_{\text{C=O}}$ vibration at $\sim 1725\text{ cm}^{-1}$, consistent with the presence of the ester carbonyl group of the *O*-benzoylsalicylate ligand.

Acknowledgements

The authors thank the University of Montana X-ray diffraction core facility (Orion Berryman and Daniel Decato) for assistance.

Funding information

Funding for this research was provided by: National Science Foundation (award Nos. CHE-0848858 and CHE-1301092).

References

Allred, R. A., McAlexander, L. H., Arif, A. M. & Berreau, L. M. (2002). *Inorg. Chem.* **41**, 6790–6801.
 Altomare, A., Burla, M. C., Camalli, M., Casciarano, G. L., Giacovazzo, C., Guagliardi, A., Moliterni, A. G. G., Polidori, G. & Spagna, R. (1999). *J. Appl. Cryst.* **32**, 115–119.
 Amatori, S., Ambrosi, G., Fanelli, M., Formica, M., Fusi, V., Giorgi, L., Macedi, E., Micheloni, M., Paoli, P. & Rossi, P. (2014). *Chem. Eur. J.* **20**, 11048–11057.
 Anderson, S. N., Noble, M., Grubel, K., Marshall, B., Arif, A. M. & Berreau, L. M. (2014). *J. Coord. Chem.* **67**, 4061–4075.
 Balogh-Hergovich, E., Kaizer, J., Speier, G., Argay, G. & Parkanyi, L. (1999). *J. Chem. Soc. Dalton Trans.* pp. 3847–3854.

Balogh-Hergovich, E., Kaizer, J., Speier, G., Fülöp, V. & Parkanyi, L. (1999). *Inorg. Chem.* **38**, 3787–3795.
 Balogh-Hergovich, E., Speier, G. & Argay, G. (1991). *Chem. Commun.* pp. 551–552.
 Benelli, C., Borgogelli, E., Formica, M., Fusi, V., Giorgi, L., Macedi, E., Micheloni, M., Paoli, P. & Rossi, P. (2013). *Dalton Trans.* **42**, 5848–5859.
 Bondi, A. (1964). *J. Phys. Chem.* **68**, 441–451.
 Burla, M. C., Caliandro, R., Camalli, M., Carrozzini, B., Casciarano, G. L., De Caro, L., Giacovazzo, C., Polidori, G. & Spagna, R. (2005). *J. Appl. Cryst.* **38**, 381–388.
 Dolomanov, O. V., Bourhis, L. J., Gildea, R. J., Howard, J. A. K. & Puschmann, H. (2009). *J. Appl. Cryst.* **42**, 339–341.
 Farrugia, L. J. (2012). *J. Appl. Cryst.* **45**, 849–854.
 Grubel, K., Laughlin, B. J., Maltais, T. R., Smith, R. C., Arif, A. M. & Berreau, L. M. (2011). *Chem. Commun.* **47**, 10431–10433.
 Grubel, K., Rudzka, K., Arif, A. M., Klotz, K. L., Halfen, J. A. & Berreau, L. M. (2010). *Inorg. Chem.* **49**, 82–96.
 Grubel, K., Saraf, S. L., Anderson, S. N., Laughlin, B. J., Smith, R. C., Arif, A. M. & Berreau, L. M. (2013). *Inorg. Chim. Acta*, **407**, 91–97.
 Hatchard, C. G. & Parker, C. A. (1956). *Proc. R. Soc. London Ser. A*, **235**, 518–536.
 Hooft, R. W. W. (1998). *COLLECT*. Nonius BV, Delft, The Netherlands.
 Huang, Q.-Q., Sun, Y.-J., Wu, H.-W. & Wang, Y.-L. (2017). *Inorg. Chim. Acta*, **467**, 7–10.
 Hunter, C. A. & Sanders, J. K. M. (1990). *J. Am. Chem. Soc.* **112**, 5525–5534.
 Janiak, C. (2000). *J. Chem. Soc. Dalton Trans.* pp. 3885–3896.
 Kaizer, J., Pap, J., Speier, G. & Parkanyi, L. (2004). *Eur. J. Inorg. Chem.* pp. 2253–2259.
 Kasprzak, M. M., Erxleben, A. & Ochocki, J. (2015). *RSC Adv.* **5**, 45853–45877.
 Kuhn, H. J., Braslavsky, S. E. & Schmidt, R. (2004). *Pure Appl. Chem.* **76**, 2105–2146.
 Kurzwernhart, A., Kandioller, W., Bächler, S., Bartel, C., Martic, S., Buczkowska, M., Mühlgassner, G., Jakupec, M. A., Kraatz, H.-B., Bednarski, P. J., Arion, V. B., Marko, D., Keppler, B. K. & Hartinger, C. G. (2012). *J. Med. Chem.* **55**, 10512–10522.
 Kurzwernhart, A., Kandioller, W., Bartel, C., Bächler, S., Trondl, R., Mühlgassner, G., Jakupec, M. A., Arion, V. B., Marko, D., Keppler, B. K. & Hartinger, C. G. (2012). *Chem. Commun.*, **48**, 4839–4841.
 Kurzwernhart, A., Kandioller, W., Enyedy, E. A., Novak, M., Jakupec, M. A., Keppler, B. K. & Hartinger, C. G. (2013). *Dalton Trans.* **42**, 6193–6202.
 Lippai, I., Speier, G., Huttner, G. & Zsolnai, L. (1997). *Acta Cryst.* **C53**, 1547–1549.
 Otwinowski, Z. & Minor, W. (1997). *Methods in Enzymology*, Vol. 276, *Macromolecular Crystallography*, Part A, edited by C. W. Carter Jr & R. M. Sweet, pp. 307–326. New York: Academic Press.
 Pap, J. S., Kaizer, J. & Speier, G. (2010). *Coord. Chem. Rev.* **254**, 781–793.
 Petrus, R., Petrus, J., Paszek, K. & Sobota, P. (2013). *Acta Cryst.* **E69**, m281–m282.
 Petrus, R. & Sobota, P. (2012a). *Acta Cryst.* **C68**, m275–m280.
 Petrus, R. & Sobota, P. (2012b). *Organometallics*, **31**, 4755–4762.
 Pieniazek, E., Kalembkiewicz, J., Dranka, M. & Woznicka, E. (2014). *J. Inorg. Biochem.* **141**, 180–187.
 Popova, M., Soboleva, T., Arif, A. M. & Berreau, L. M. (2017). *RSC Adv.* **7**, 21997–22007.
 Saraf, S. L., Fish, T. J., Benninghoff, A. D., Buelt, A. A., Smith, R. C. & Berreau, L. M. (2014). *Organometallics*, **33**, 6341–6351.
 Schutte, M., Kemp, G., Visser, H. G. & Roodt, A. (2011). *Inorg. Chem.* **50**, 12486–12498.
 Sheldrick, G. M. (2015). *Acta Cryst.* **C71**, 3–8.
 Souza, R. F. V. de & de Giovani, W. F. (2004). *Redox Rep.* **9**, 97–104.

- Speier, G., Fülöp, V. & Parkanyi, L. (1990). *Chem. Commun.* pp. 512–513.
- Sun, Y.-J., Huang, Q.-Q., Tano, T. & Itoh, S. (2013). *Inorg. Chem.* **52**, 10936–10948.
- Sun, Y.-J., Huang, Q.-Q. & Zhang, J.-J. (2014a). *Inorg. Chem.* **53**, 2932–2942.
- Sun, Y.-J., Huang, Q.-Q. & Zhang, J.-J. (2014b). *Dalton Trans.* **43**, 6480–6489.
- Sun, Y.-J., Li, P., Huang, Q.-Q., Zhang, J. J. & Itoh, S. (2017). *Eur. J. Inorg. Chem.* pp. 1845–1854.
- Szajna, E., Dobrowolski, P., Fuller, A. L., Arif, A. M. & Berreau, L. M. (2004). *Inorg. Chem.* **43**, 3988–3997.
- Vijayaraghavan, K., Pillai, S. I. & Subramanian, S. P. (2012). *Eur. J. Pharmacol.* **680**, 122–129.
- Wei, Y. & Guo, M. (2014). *Biol. Trace Elem. Res.* **161**, 223–230.
- Wolsey, W. C. (1973). *J. Chem. Educ.* **50**, A335.

supporting information

Acta Cryst. (2017). **C73**, 703-709 [https://doi.org/10.1107/S2053229617011366]

A bipyridine-ligated zinc(II) complex with bridging flavonolate ligation: synthesis, characterization, and visible-light-induced CO release reactivity

Shayne Sorenson, Marina Popova, Atta M. Arif and Lisa M. Berreau

Computing details

Data collection: *COLLECT* (Hooft, 1998); cell refinement: *DENZO-SMN* (Otwinowski & Minor, 1997) and *SIR97* (Altomare *et al.*, 1999); data reduction: *DENZO-SMN* (Otwinowski & Minor, 1997); program(s) used to solve structure: *SIR2004* (Burla *et al.*, 2007); program(s) used to refine structure: *SHELXL2014* (Sheldrick, 2015); molecular graphics: *OLEX2* (Dolomanov *et al.*, 2009) and *ORTEP-3 for Windows* (Farrugia, 2012); software used to prepare material for publication: *OLEX2* (Dolomanov *et al.*, 2009).

Bis(μ -4-oxo-2-phenyl-4H-chromen-3-olato)- κ^3 O³:O³,O⁴; κ^3 O³,O⁴:O³-bis[(2,2'-bipyridine- κ^2 N,N')zinc(II)] bis(perchlorate)

Crystal data

[Zn₂(C₁₅H₉O₃)₂(C₁₀H₈N₂)₂](ClO₄)₂

$M_r = 1116.45$

Monoclinic, $P2_1/n$

$a = 10.6003$ (2) Å

$b = 14.0573$ (3) Å

$c = 15.8141$ (2) Å

$\beta = 104.0158$ (10)°

$V = 2286.33$ (7) Å³

$Z = 2$

$F(000) = 1136$

$D_x = 1.622$ Mg m⁻³

Mo $K\alpha$ radiation, $\lambda = 0.71073$ Å

Cell parameters from 5179 reflections

$\theta = 1.0$ – 27.5°

$\mu = 1.24$ mm⁻¹

$T = 150$ K

Prism, yellow

$0.28 \times 0.25 \times 0.20$ mm

Data collection

Nonius KappaCCD
diffractometer

Radiation source: fine-focus sealed tube

Phi and ω scan

Absorption correction: multi-scan

(DENZO-SMN; Otwinowski & Minor, 1997)

$T_{\min} = 0.722$, $T_{\max} = 0.789$

8971 measured reflections

5225 independent reflections

4417 reflections with $I > 2\sigma(I)$

$R_{\text{int}} = 0.016$

$\theta_{\max} = 27.5^\circ$, $\theta_{\min} = 2.5^\circ$

$h = -13 \rightarrow 13$

$k = -16 \rightarrow 18$

$l = -20 \rightarrow 20$

Refinement

Refinement on F^2

Least-squares matrix: full

$R[F^2 > 2\sigma(F^2)] = 0.037$

$wR(F^2) = 0.093$

$S = 1.03$

5225 reflections

341 parameters

28 restraints

Primary atom site location: structure-invariant
direct methods

Hydrogen site location: inferred from
neighbouring sites

H-atom parameters constrained

$$w = 1/[\sigma^2(F_o^2) + (0.038P)^2 + 2.5961P]$$

where $P = (F_o^2 + 2F_c^2)/3$
 $(\Delta/\sigma)_{\max} = 0.001$

$$\Delta\rho_{\max} = 1.06 \text{ e } \text{\AA}^{-3}$$

$$\Delta\rho_{\min} = -0.51 \text{ e } \text{\AA}^{-3}$$

Special details

Experimental. The program Denzo-SMN (Otwinowski & Minor, 1997) uses a scaling algorithm (Fox & Holmes, 1966) which effectively corrects for absorption effects. High redundancy data were used in the scaling program hence the 'multi-scan' code word was used. No transmission coefficients are available from the program (only scale factors for each frame). The scale factors in the experimental table are calculated from the 'size' command in the SHELXL-97 input file.

Geometry. All esds (except the esd in the dihedral angle between two l.s. planes) are estimated using the full covariance matrix. The cell esds are taken into account individually in the estimation of esds in distances, angles and torsion angles; correlations between esds in cell parameters are only used when they are defined by crystal symmetry. An approximate (isotropic) treatment of cell esds is used for estimating esds involving l.s. planes.

Fractional atomic coordinates and isotropic or equivalent isotropic displacement parameters (\AA^2)

	<i>x</i>	<i>y</i>	<i>z</i>	$U_{\text{iso}}^*/U_{\text{eq}}$	Occ. (<1)
Zn1	0.63071 (2)	0.45723 (2)	0.49175 (2)	0.02410 (9)	
O1	0.50997 (14)	0.44202 (10)	0.57399 (9)	0.0211 (3)	
O2	0.54863 (16)	0.33113 (11)	0.44544 (10)	0.0281 (3)	
O3	0.36814 (17)	0.21939 (11)	0.62159 (10)	0.0299 (4)	
N1	0.76003 (18)	0.47018 (13)	0.41398 (12)	0.0234 (4)	
N2	0.75846 (17)	0.55667 (13)	0.56275 (11)	0.0216 (4)	
C1	0.4701 (2)	0.35118 (15)	0.57078 (13)	0.0215 (4)	
C2	0.4885 (2)	0.29575 (15)	0.49750 (14)	0.0238 (4)	
C3	0.4322 (2)	0.20209 (16)	0.48603 (15)	0.0274 (5)	
C4	0.4304 (3)	0.14514 (17)	0.41248 (16)	0.0339 (5)	
H4	0.4686	0.1678	0.3679	0.041*	
C5	0.3734 (3)	0.05677 (19)	0.40522 (18)	0.0410 (6)	
H5	0.3722	0.0185	0.3555	0.049*	
C6	0.3169 (3)	0.02282 (19)	0.47094 (19)	0.0421 (6)	
H6	0.2794	-0.0389	0.4659	0.050*	
C7	0.3152 (3)	0.07794 (19)	0.54257 (17)	0.0389 (6)	
H7	0.2757	0.0553	0.5866	0.047*	
C8	0.3727 (2)	0.16787 (17)	0.54928 (15)	0.0296 (5)	
C9	0.4154 (2)	0.31063 (15)	0.63192 (14)	0.0240 (4)	
C10	0.4020 (2)	0.35302 (16)	0.71466 (14)	0.0262 (5)	
C11	0.4834 (3)	0.42693 (18)	0.75412 (15)	0.0323 (5)	
H11	0.5430	0.4544	0.7249	0.039*	
C12	0.4778 (3)	0.46066 (19)	0.83612 (16)	0.0382 (6)	
H12	0.5327	0.5114	0.8622	0.046*	
C13	0.3928 (3)	0.4203 (2)	0.87918 (16)	0.0409 (6)	
H13	0.3919	0.4415	0.9361	0.049*	
C14	0.3090 (3)	0.3495 (2)	0.84028 (17)	0.0398 (6)	
H14	0.2492	0.3232	0.8699	0.048*	
C15	0.3115 (2)	0.31615 (18)	0.75770 (16)	0.0310 (5)	
H15	0.2519	0.2684	0.7306	0.037*	
C16	0.7600 (2)	0.41937 (18)	0.34236 (16)	0.0319 (5)	
H16	0.6993	0.3689	0.3263	0.038*	

C17	0.8460 (3)	0.43842 (19)	0.29110 (16)	0.0356 (6)	
H17	0.8446	0.4014	0.2407	0.043*	
C18	0.9335 (2)	0.51187 (19)	0.31430 (16)	0.0327 (5)	
H18	0.9930	0.5263	0.2798	0.039*	
C19	0.9338 (2)	0.56433 (17)	0.38805 (15)	0.0275 (5)	
H19	0.9936	0.6151	0.4051	0.033*	
C20	0.8458 (2)	0.54196 (15)	0.43692 (13)	0.0206 (4)	
C21	0.8386 (2)	0.59469 (16)	0.51706 (13)	0.0209 (4)	
C22	0.9060 (2)	0.67780 (18)	0.54329 (15)	0.0287 (5)	
H22	0.9606	0.7045	0.5099	0.034*	
C23	0.8929 (2)	0.72163 (19)	0.61922 (16)	0.0353 (6)	
H23	0.9373	0.7795	0.6378	0.042*	
C24	0.8148 (2)	0.68084 (19)	0.66787 (15)	0.0344 (6)	
H24	0.8073	0.7087	0.7212	0.041*	
C25	0.7484 (2)	0.59883 (18)	0.63707 (14)	0.0286 (5)	
H25	0.6934	0.5710	0.6696	0.034*	
Cl1A	0.8773 (6)	0.2224 (3)	0.6510 (4)	0.0346 (2)	0.176 (2)
O4A	0.8000 (14)	0.1459 (9)	0.6684 (9)	0.0532 (7)	0.176 (2)
O5A	0.8154 (13)	0.3096 (9)	0.6666 (13)	0.0697 (9)	0.176 (2)
O6A	0.9914 (17)	0.2401 (16)	0.7179 (12)	0.0824 (12)	0.176 (2)
O7A	0.9252 (19)	0.204 (2)	0.5791 (11)	0.0714 (13)	0.176 (2)
Cl1	0.82388 (10)	0.24761 (7)	0.62407 (6)	0.0346 (2)	0.824 (2)
O4	0.7164 (3)	0.18804 (19)	0.63012 (18)	0.0532 (7)	0.824 (2)
O5	0.7794 (3)	0.3426 (2)	0.6089 (3)	0.0697 (9)	0.824 (2)
O6	0.9246 (4)	0.2448 (3)	0.7016 (2)	0.0824 (12)	0.824 (2)
O7	0.8706 (3)	0.2153 (4)	0.5529 (2)	0.0714 (13)	0.824 (2)

Atomic displacement parameters (\AA^2)

	U^{11}	U^{22}	U^{33}	U^{12}	U^{13}	U^{23}
Zn1	0.02362 (14)	0.01885 (14)	0.03314 (15)	-0.00616 (10)	0.01330 (10)	-0.00421 (10)
O1	0.0244 (7)	0.0154 (7)	0.0250 (7)	-0.0041 (6)	0.0088 (6)	0.0008 (6)
O2	0.0371 (9)	0.0208 (8)	0.0307 (8)	-0.0088 (7)	0.0166 (7)	-0.0038 (6)
O3	0.0450 (10)	0.0189 (8)	0.0281 (8)	-0.0085 (7)	0.0135 (7)	0.0042 (6)
N1	0.0225 (9)	0.0212 (9)	0.0277 (9)	0.0006 (7)	0.0083 (7)	-0.0030 (7)
N2	0.0215 (9)	0.0224 (9)	0.0217 (8)	-0.0049 (7)	0.0066 (7)	0.0011 (7)
C1	0.0237 (10)	0.0169 (10)	0.0235 (10)	-0.0007 (8)	0.0051 (8)	0.0030 (8)
C2	0.0280 (11)	0.0191 (11)	0.0247 (10)	-0.0028 (9)	0.0073 (9)	0.0021 (8)
C3	0.0330 (12)	0.0185 (11)	0.0306 (11)	-0.0053 (9)	0.0076 (9)	0.0007 (9)
C4	0.0425 (14)	0.0242 (12)	0.0372 (13)	-0.0076 (11)	0.0140 (11)	-0.0047 (10)
C5	0.0532 (17)	0.0270 (14)	0.0439 (15)	-0.0112 (12)	0.0141 (13)	-0.0108 (11)
C6	0.0549 (17)	0.0228 (13)	0.0485 (15)	-0.0158 (12)	0.0127 (13)	-0.0018 (11)
C7	0.0546 (16)	0.0255 (13)	0.0383 (13)	-0.0153 (12)	0.0146 (12)	0.0042 (11)
C8	0.0387 (13)	0.0201 (11)	0.0296 (12)	-0.0055 (10)	0.0077 (10)	0.0017 (9)
C9	0.0292 (11)	0.0167 (10)	0.0256 (10)	-0.0014 (9)	0.0061 (9)	0.0040 (8)
C10	0.0328 (12)	0.0223 (11)	0.0238 (10)	0.0070 (9)	0.0075 (9)	0.0083 (9)
C11	0.0426 (14)	0.0282 (12)	0.0254 (11)	0.0015 (11)	0.0066 (10)	0.0042 (9)
C12	0.0497 (16)	0.0329 (14)	0.0287 (12)	0.0109 (12)	0.0031 (11)	-0.0008 (10)

C13	0.0493 (16)	0.0460 (16)	0.0277 (12)	0.0247 (14)	0.0101 (11)	0.0028 (11)
C14	0.0409 (14)	0.0472 (16)	0.0381 (13)	0.0206 (13)	0.0227 (12)	0.0125 (12)
C15	0.0311 (12)	0.0299 (13)	0.0342 (12)	0.0093 (10)	0.0121 (10)	0.0090 (10)
C16	0.0337 (12)	0.0265 (12)	0.0363 (12)	0.0025 (10)	0.0100 (10)	-0.0094 (10)
C17	0.0411 (14)	0.0385 (15)	0.0297 (12)	0.0115 (11)	0.0138 (11)	-0.0055 (10)
C18	0.0322 (12)	0.0389 (14)	0.0319 (12)	0.0097 (11)	0.0172 (10)	0.0064 (10)
C19	0.0235 (11)	0.0315 (13)	0.0288 (11)	0.0012 (9)	0.0089 (9)	0.0062 (9)
C20	0.0198 (10)	0.0195 (10)	0.0227 (10)	0.0022 (8)	0.0055 (8)	0.0029 (8)
C21	0.0195 (10)	0.0225 (11)	0.0208 (9)	-0.0015 (8)	0.0051 (8)	0.0040 (8)
C22	0.0266 (11)	0.0310 (13)	0.0285 (11)	-0.0095 (10)	0.0071 (9)	0.0000 (10)
C23	0.0347 (13)	0.0357 (14)	0.0341 (13)	-0.0144 (11)	0.0055 (10)	-0.0108 (11)
C24	0.0354 (13)	0.0420 (15)	0.0259 (11)	-0.0061 (11)	0.0077 (10)	-0.0100 (10)
C25	0.0283 (11)	0.0354 (13)	0.0239 (10)	-0.0051 (10)	0.0096 (9)	-0.0005 (9)
Cl1A	0.0377 (5)	0.0353 (5)	0.0355 (5)	-0.0105 (4)	0.0178 (4)	-0.0056 (3)
O4A	0.0634 (18)	0.0483 (16)	0.0586 (16)	-0.0300 (13)	0.0354 (14)	-0.0149 (12)
O5A	0.0449 (16)	0.0405 (16)	0.117 (3)	-0.0064 (13)	0.0076 (17)	0.0004 (17)
O6A	0.080 (3)	0.089 (2)	0.059 (2)	-0.026 (3)	-0.021 (2)	0.0048 (18)
O7A	0.078 (3)	0.085 (2)	0.070 (2)	-0.025 (3)	0.054 (2)	-0.027 (2)
Cl1	0.0377 (5)	0.0353 (5)	0.0355 (5)	-0.0105 (4)	0.0178 (4)	-0.0056 (3)
O4	0.0634 (18)	0.0483 (16)	0.0586 (16)	-0.0300 (13)	0.0354 (14)	-0.0149 (12)
O5	0.0449 (16)	0.0405 (16)	0.117 (3)	-0.0064 (13)	0.0076 (17)	0.0004 (17)
O6	0.080 (3)	0.089 (2)	0.059 (2)	-0.026 (3)	-0.021 (2)	0.0048 (18)
O7	0.078 (3)	0.085 (2)	0.070 (2)	-0.025 (3)	0.054 (2)	-0.027 (2)

Geometric parameters (Å, °)

Zn1—O1	2.0448 (14)	C12—H12	0.9500
Zn1—O2	2.0315 (16)	C12—C13	1.377 (4)
Zn1—O1 ⁱ	2.1353 (15)	C13—H13	0.9500
Zn1—N1	2.0595 (18)	C13—C14	1.376 (4)
Zn1—N2	2.0765 (18)	C14—H14	0.9500
Zn1—Zn1 ⁱ	3.0891 (5)	C14—C15	1.394 (4)
O1—Zn1 ⁱ	2.1352 (15)	C15—H15	0.9500
O1—C1	1.342 (3)	C16—H16	0.9500
O2—C2	1.259 (3)	C16—C17	1.385 (3)
O3—C8	1.364 (3)	C17—H17	0.9500
O3—C9	1.372 (3)	C17—C18	1.377 (4)
N1—C16	1.339 (3)	C18—H18	0.9500
N1—C20	1.348 (3)	C18—C19	1.379 (3)
N2—C21	1.351 (3)	C19—H19	0.9500
N2—C25	1.343 (3)	C19—C20	1.384 (3)
C1—C2	1.448 (3)	C20—C21	1.486 (3)
C1—C9	1.367 (3)	C21—C22	1.380 (3)
C2—C3	1.439 (3)	C22—H22	0.9500
C3—C4	1.408 (3)	C22—C23	1.386 (3)
C3—C8	1.391 (3)	C23—H23	0.9500
C4—H4	0.9500	C23—C24	1.383 (3)
C4—C5	1.374 (3)	C24—H24	0.9500

C5—H5	0.9500	C24—C25	1.377 (3)
C5—C6	1.403 (4)	C25—H25	0.9500
C6—H6	0.9500	C11A—O4A	1.419 (10)
C6—C7	1.376 (4)	C11A—O5A	1.440 (11)
C7—H7	0.9500	C11A—O6A	1.422 (11)
C7—C8	1.396 (3)	C11A—O7A	1.377 (13)
C9—C10	1.476 (3)	C11—O4	1.436 (2)
C10—C11	1.398 (3)	C11—O5	1.417 (3)
C10—C15	1.403 (3)	C11—O6	1.418 (3)
C11—H11	0.9500	C11—O7	1.410 (3)
C11—C12	1.395 (3)		
O2—Zn1—O1	81.87 (6)	C10—C11—H11	119.8
O2—Zn1—N1	98.67 (7)	C12—C11—C10	120.5 (2)
O1—Zn1—N1	177.08 (7)	C12—C11—H11	119.8
O2—Zn1—N2	161.55 (7)	C11—C12—H12	120.0
O1—Zn1—N2	98.81 (6)	C13—C12—C11	120.0 (3)
N1—Zn1—N2	79.76 (7)	C13—C12—H12	120.0
O2—Zn1—O1 ⁱ	102.45 (6)	C12—C13—H13	119.8
O1—Zn1—O1 ⁱ	84.73 (6)	C14—C13—C12	120.4 (2)
N1—Zn1—O1 ⁱ	97.93 (6)	C14—C13—H13	119.8
N2—Zn1—O1 ⁱ	95.96 (6)	C13—C14—H14	119.8
O1—Zn1—Zn1 ⁱ	43.49 (4)	C13—C14—C15	120.4 (2)
O1 ⁱ —Zn1—Zn1 ⁱ	41.23 (4)	C15—C14—H14	119.8
O1—Zn1—N2	98.81 (6)	C10—C15—H15	120.0
O2—Zn1—Zn1 ⁱ	93.18 (5)	C14—C15—C10	120.0 (3)
N1—Zn1—Zn1 ⁱ	139.15 (5)	C14—C15—H15	120.0
N2—Zn1—Zn1 ⁱ	99.97 (5)	N1—C16—H16	119.1
Zn1—O1—Zn1 ⁱ	95.27 (6)	N1—C16—C17	121.8 (2)
C1—O1—Zn1	108.39 (12)	C17—C16—H16	119.1
C1—O1—Zn1 ⁱ	115.85 (13)	C16—C17—H17	120.5
C2—O2—Zn1	110.45 (14)	C18—C17—C16	119.0 (2)
C8—O3—C9	120.67 (17)	C18—C17—H17	120.5
C16—N1—Zn1	126.44 (16)	C17—C18—H18	120.3
C16—N1—C20	119.29 (19)	C17—C18—C19	119.3 (2)
C20—N1—Zn1	114.12 (14)	C19—C18—H18	120.3
C21—N2—Zn1	112.90 (14)	C18—C19—H19	120.4
C25—N2—Zn1	126.19 (15)	C18—C19—C20	119.1 (2)
C25—N2—C21	119.11 (19)	C20—C19—H19	120.4
O1—C1—C2	116.09 (18)	N1—C20—C19	121.5 (2)
O1—C1—C9	123.63 (19)	N1—C20—C21	115.60 (18)
C9—C1—C2	120.3 (2)	C19—C20—C21	122.9 (2)
O2—C2—C1	119.88 (19)	N2—C21—C20	115.31 (18)
O2—C2—C3	122.6 (2)	N2—C21—C22	121.4 (2)
C3—C2—C1	117.46 (19)	C22—C21—C20	123.26 (19)
C4—C3—C2	123.1 (2)	C21—C22—H22	120.6
C8—C3—C2	118.2 (2)	C21—C22—C23	118.9 (2)
C8—C3—C4	118.6 (2)	C23—C22—H22	120.6

C3—C4—H4	120.0	C22—C23—H23	120.1
C5—C4—C3	120.1 (2)	C24—C23—C22	119.8 (2)
C5—C4—H4	120.0	C24—C23—H23	120.1
C4—C5—H5	119.9	C23—C24—H24	120.9
C4—C5—C6	120.2 (2)	C25—C24—C23	118.3 (2)
C6—C5—H5	119.9	C25—C24—H24	120.9
C5—C6—H6	119.6	N2—C25—C24	122.5 (2)
C7—C6—C5	120.7 (2)	N2—C25—H25	118.8
C7—C6—H6	119.6	C24—C25—H25	118.8
C6—C7—H7	120.7	O4A—C11A—O5A	107.6 (9)
C6—C7—C8	118.7 (2)	O4A—C11A—O6A	114.5 (11)
C8—C7—H7	120.7	O6A—C11A—O5A	93.7 (12)
O3—C8—C3	122.2 (2)	O7A—C11A—O4A	111.2 (13)
O3—C8—C7	116.2 (2)	O7A—C11A—O5A	125.4 (15)
C3—C8—C7	121.6 (2)	O7A—C11A—O6A	103.3 (14)
O3—C9—C10	111.86 (18)	O5—C11—O4	108.93 (18)
C1—C9—O3	120.71 (19)	O5—C11—O6	108.8 (2)
C1—C9—C10	127.4 (2)	O6—C11—O4	111.7 (2)
C11—C10—C9	121.0 (2)	O7—C11—O4	107.7 (2)
C11—C10—C15	118.6 (2)	O7—C11—O5	109.6 (3)
C15—C10—C9	120.3 (2)	O7—C11—O6	110.2 (2)
Zn1 ⁱ —O1—C1—C2	89.22 (19)	C4—C5—C6—C7	1.4 (5)
Zn1—O1—C1—C2	-16.4 (2)	C5—C6—C7—C8	-1.0 (4)
Zn1 ⁱ —O1—C1—C9	-91.0 (2)	C6—C7—C8—O3	180.0 (2)
Zn1—O1—C1—C9	163.38 (18)	C6—C7—C8—C3	-0.6 (4)
Zn1—O2—C2—C1	8.7 (3)	C8—O3—C9—C1	-1.2 (3)
Zn1—O2—C2—C3	-173.41 (18)	C8—O3—C9—C10	-179.5 (2)
Zn1—N1—C16—C17	175.30 (18)	C8—C3—C4—C5	-1.5 (4)
Zn1—N1—C20—C19	-175.72 (16)	C9—O3—C8—C3	4.3 (3)
Zn1—N1—C20—C21	4.0 (2)	C9—O3—C8—C7	-176.3 (2)
Zn1—N2—C21—C20	-15.7 (2)	C9—C1—C2—O2	-174.1 (2)
Zn1—N2—C21—C22	163.08 (17)	C9—C1—C2—C3	7.9 (3)
Zn1—N2—C25—C24	-162.27 (19)	C9—C10—C11—C12	-174.2 (2)
O1—C1—C2—O2	5.6 (3)	C9—C10—C15—C14	173.0 (2)
O1—C1—C2—C3	-172.35 (19)	C10—C11—C12—C13	0.8 (4)
O1—C1—C9—O3	175.31 (19)	C11—C10—C15—C14	-3.6 (3)
O1—C1—C9—C10	-6.6 (4)	C11—C12—C13—C14	-2.8 (4)
O2—C2—C3—C4	-5.2 (4)	C12—C13—C14—C15	1.6 (4)
O2—C2—C3—C8	177.2 (2)	C13—C14—C15—C10	1.6 (4)
O3—C9—C10—C11	155.6 (2)	C15—C10—C11—C12	2.4 (3)
O3—C9—C10—C15	-20.9 (3)	C16—N1—C20—C19	0.0 (3)
N1—C16—C17—C18	-0.3 (4)	C16—N1—C20—C21	179.8 (2)
N1—C20—C21—N2	8.0 (3)	C16—C17—C18—C19	0.3 (4)
N1—C20—C21—C22	-170.8 (2)	C17—C18—C19—C20	-0.2 (4)
N2—C21—C22—C23	1.4 (3)	C18—C19—C20—N1	0.0 (3)
C1—C2—C3—C4	172.7 (2)	C18—C19—C20—C21	-179.7 (2)
C1—C2—C3—C8	-4.9 (3)	C19—C20—C21—N2	-172.3 (2)

C1—C9—C10—C11	-22.6 (4)	C19—C20—C21—C22	9.0 (3)
C1—C9—C10—C15	160.9 (2)	C20—N1—C16—C17	0.1 (3)
C2—C1—C9—O3	-5.0 (3)	C20—C21—C22—C23	-179.9 (2)
C2—C1—C9—C10	173.1 (2)	C21—N2—C25—C24	1.4 (3)
C2—C3—C4—C5	-179.1 (2)	C21—C22—C23—C24	1.1 (4)
C2—C3—C8—O3	-1.0 (4)	C22—C23—C24—C25	-2.3 (4)
C2—C3—C8—C7	179.6 (2)	C23—C24—C25—N2	1.1 (4)
C3—C4—C5—C6	-0.1 (4)	C25—N2—C21—C20	178.60 (19)
C4—C3—C8—O3	-178.7 (2)	C25—N2—C21—C22	-2.6 (3)
C4—C3—C8—C7	1.9 (4)		

Symmetry code: (i) $-x+1, -y+1, -z+1$.